New Hybrid System: Poly(ethylene glycol) Hydrogel with Covalently Bonded Pegylated Nanotubes

Virginia Saez-Martinez, Ainara Garcia-Gallastegui, Carolina Vera, Beatriz Olalde, Iratxe Madarieta, Isabel Obieta, Nerea Garagorri

Health Unit, Inasmet-Tecnalia, Paseo Mikeletegui 2, Donostia-San Sebastián, Spain 20009

Received 12 January 2010; accepted 25 July 2010
DOI 10.1002/app.33095
Published online 11 October 2010 in Wiley Online Library (wileyonlinelibrary.com).

ABSTRACT: Hydrogels containing carbon nanotubes (CNTs) are expected to be promising conjugates because they might show a synergic combination of properties from both materials. Most of the hybrid materials containing CNTs only entrap them physically, and the covalent attachment has not been properly addressed yet. In this study, single-walled carbon nanotubes (SWNTs) were successfully incorporated into a poly(ethylene glycol) (PEG) hydrogel by covalent bonds to form a hybrid material. For this purpose, SWNTs were functionalized with poly(ethylene glycol) methacrylate (PEGMA) to obtain water-soluble pegylated SWNTs (SWNT–PEGMA). These functionalized SWNTs were covalently bonded through their PEG moieties to a PEG hydrogel. The hybrid network was obtained from the crosslinking reaction of poly(ethylene glycol) diacrylate prepolymer and the SWNT–PEGMA by dual photo-UV and thermal initiations. The mechanical and swelling properties of the new hybrid material were studied. In addition, the material and lixiviates were analyzed to elucidate any kind of SWNT release and to evaluate a possible *in vitro* cytotoxic effect. © 2010 Wiley Periodicals, Inc. J Appl Polym Sci 120: 124–132, 2011

Key words: hydrogels; mechanical properties; nanocomposites; swelling

INTRODUCTION

Carbon nanotubes (CNTs) are being broadly investigated in biomedical fields,[1,2] mainly in bioelectronics, in drug-delivery systems, and as reinforcements and additives in biomaterials. In this context, composite materials based on CNTs are already being studied and are expected to show challenging possibilities.[3]

More concretely, hydrogels that incorporate CNTs are very promising materials because they can combine two or more separate domains of very different natures to produce novel structures with new properties.

The mechanical properties of single-walled carbon nanotubes (SWNTs), with an estimated Young's modulus of 1 TPa,[4] make them extremely attractive for polymer reinforcement, especially in the case of soft materials, such as hydrogels. The advantages of hydrogels as biomaterials lie in their high permeability, their elasticity, and their low interfacial tension with aqueous solutions. These physical properties are very similar to those of living tissues.[5–8] They can be used as contact lenses, membranes, controlled drug-release systems, and soft tissue substitutes and in some other tissue engineering applications.[9–12] For example, hydrogels obtained by photocrosslinking have been investigated for several tissue engineering applications because of their ability to be formed *in situ* in a minimally invasive manner and in the presence of living cells.[13,14]

One of the most extensively used polymers for clinical use is poly(ethylene glycol) (PEG) and its derivatives because of its biocompatibility and lack of toxicity.[15–17] This hydrophilic polymer can be acrylated to produce prepolymers, such as poly(ethylene glycol) dimethacrylate (PEGDMA) or poly(ethylene glycol) diacrylate (PEGDA), that form crosslinked networks by a photocrosslinking reaction with a suitable photoinitiator.[18–20]

In addition, the functionalization of CNTs with covalently bonded hydrophilic polymers, such as the PEG usually used as a raw material in hydrogels, improves the dispersion of the CNTs in water media. The most extended strategy for covalent attachment is through an ester bond between the carboxylated CNTs and the hydroxyl terminal group of the polymer.[21–24]

For all these reasons, we search after hydrogels hybridized with CNTs for bio-inspired applications. Some researches have reported gelation processes of some CNT preparations, but these gels were not

Correspondence to: V. Saez-Martinez (vsaez@inasmet.es).
Contract grant sponsor: Basque Department of Industry (through SAIOTEK); contract grant numbers: S-PE06IN07 and S-PE06IN10.
Contract grant sponsor: Spanish Ministry of Education and Science; contract grant number: PSE-300100-2006-1.

physically consistent enough and could dissolve very easily.[25] Other authors have reported the formation of CNT–polymer composites and hydrogels where the CNTs were physically entrapped in the material.[26–29] In other cases, they could move easily to the medium outside because of weak van der Waals interactions between the CNTs and the polymer matrix.[30–32] Although less extended,[33–35] the covalent chemistry proposed herein is an alternative method for obtaining a stable attachment between SWNTs and the crosslinked hydrogel. However, the presence of SWNTs during the crosslinking reaction had a drawback: their opacity could hinder the photopolymerization reaction, and this fact made us think of using a dual initiation system. Photopolymerization is fast and can be used under physiological conditions, but when dark areas are present in the material, the conversion decreases, and potentially toxic material can be released. This problem can be solved by the combining of the photoinitiators with thermal initiators; this can provide synergistic advantages. Polymerization begins at the points directly exposed to UV light through photoinitiation, and then, because of the exothermic nature of this reaction, the thermal initiator is dissociated; this gives rise to a curing process and network formation in the dark areas. In this way, the two initiation mechanisms are coupled. In addition, photopolymerization can be used to gel the system initially, whereas a much slower thermally initiated polymerization can subsequently increase the network conversion over a longer timescale. Several investigations have already addressed this issue.[36,37]

In this article, we report a new strategy to functionalize SWNTs with PEGMA after a previous two-step oxidation/esterification process. The obtained pegylated nanotubes (SWNT–PEGMA) were covalently bound through their PEG moieties to a PEG hydrogel network, which was obtained from the photocrosslinking reaction of the PEGDA prepolymer by dual photo-UV and thermal initiations. When the precursor solution was irradiated under UV light, the dual initiator system initiated the polymerization of the C=C double bonds of the PEG derivatives (free PEGDA and PEGMA from SWNTs), and this led to the formation of the hybrid covalently crosslinked SWNT–PEG hydrogel systems. The material was characterized with rheological and swelling tests, and we paid special attention to the lixiviates and cytotoxicity.

EXPERIMENTAL

CNT functionalization

Materials

SWNT soot was purchased from Nanocyl (Nanocyl-1100, Sambreville, Belgium) and was used without further purification. All of the reagents were used as purchased from Sigma–Aldrich (Madrid, Spain). Filtrations were performed on polycarbonate membranes [isopore filters in policarbonate (GTTP), pore size = 0.2 μm] and fluoropore membranes with a pore size of 0.22 μm (Millipore, Madrid, Spain). Fourier transform infrared spectra were recorded on a Nicolet Magna IR 750 spectrometer (Izasa S.A., Barcelona, Spain) equipped with a monochromatic IR-ray source (Ever-Glo mid-IR) and a deuterated triglycine sulfate (DTGS)–KBr detector with dried KBr-embedded pellets. Thermogravimetric measurements were carried out on a TGA-Q500 TA Instruments (Barcelona, Spain) instrument under nitrogen flow at a scan rate of 10°C/min from 100 to 1000°C and with the temperature kept at 100 and 1000°C for 20 min. X-ray photoelectron spectroscopy measurements were made in a Microlab MK II from V. G. Scientific (Madrid, Spain). Scanning electron microscopy (SEM) observations were conducted with a JEOL JSM 5910-LV field emission source (Izasa S.A.). The Raman spectra were obtained with a Raman microscope from Renishaw (Barcelona, Spain) with a laser light wavelength of 785 nm. For atomic force microscopy (AFM) analysis, a small amount of nanotubes was dissolved in dimethylformamide (DMF), and a drop of the solution was placed on a freshly cleaved mica slide. After drying, the sample was scanned with a Multimode AFM from Veeco Digital Instruments (Cambridge, France).

Methods

Carboxyl-functionalized SWNTs were prepared by oxidation of the material.[38] Pristine SWNTs were first treated by 2.6*M* nitric acid treatment (100 mL) under stirring overnight at 120°C. After this treatment, the nanotubes were separated from the residue by filtration over a Millipore GTTP membrane (0.2 μm) and washed extensively with water and dried. Subsequently, the obtained SWNTs (100 mg) and H_2O_2–H_2SO_4 (160 : 40 mL) were mixed by stirring at 37°C for 1.5 h. After cooling to room temperature, SWNT–CO_2H was recovered from the supernatant by filtration over a Millipore fluoropore membrane (0.22 μm), washed extensively with water until complete removal of the residual acids was accomplished, and oven-dried overnight at 105°C. SWNT–CO_2H (100 mg), $SOCl_2$ (20 mL), and anhydrous DMF (1 mL) were refluxed for 24 h with stirring under a nitrogen atmosphere in a 100-mL flask equipped with a condenser.[39] After cooling to room temperature, the excess $SOCl_2$ was removed in a rotary evaporator to afford crude SWNT–COCl (100 mg). The coupling with the PEGMA (Sigma–Aldrich) was developed with the methodology previously set up for poly(L-lactic acid).[7] The SWNT–

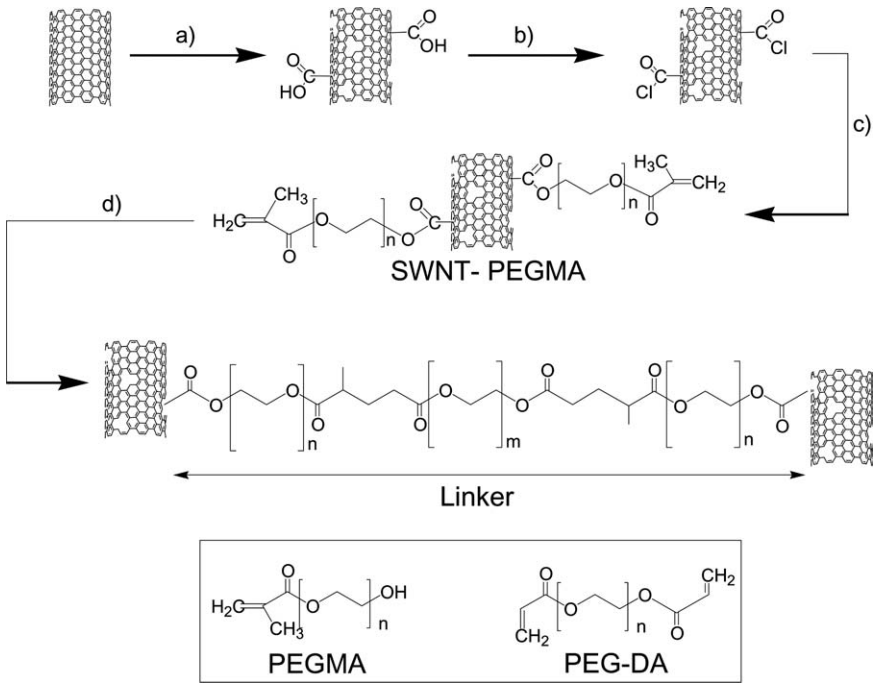

Scheme 1 Reagents and conditions: (a) H_2O_2–H_2SO_4, 37°C, and 1.5 h; (b) $SOCl_2$, DMF, 60°C, and 24 h; (c) PEGMA, Et_3N, DMF, 90°C, and 24 h; and (d) PEGDA, Irgacure 2959, KPS, water, room temperature, UV light, and 5 min.

COCl product was resuspended in a solution of PEGMA (10 mL) in anhydrous DMF (15 mL) and anhydrous triethylamine (1 mL). The mixture was stirred 24 h under an inert atmosphere at 90°C in a 100-mL flask equipped with a condenser. The SWNT–PEGMA product was recovered by vacuum filtration over a Millipore fluoropore membrane, washed extensively with DMF and ethanol, and dried *in vacuo* (see Scheme 1).

Hydrogel synthesis

Materials

PEGDA (weight-average molecular weight = 3400) was purchased from SunBio (Anyang City, South Korea) and was used as received without further purification. The photoinitiator {2-hydroxyl-1-[4-(hydroxyethoxy)phenyl]-2-methyl-1-propanone, Irgacure 2959} was supplied by Ciba Specialty Chemicals (Basel, Switzerland), and the thermal initiator potassium persulfate (KPS) was supplied by Sigma–Aldrich; both were used as received.

Methods

Previous procedures were followed to fabricate the photopolymerized hydrogels.[36,37,40,41] SWNT–PEGMA was dispersed in deionized water (MilliQ) at different concentrations and sonicated for several minutes. Then, PEGDA was added to the SWNT–PEGMA dispersion to form 20 and 30% (w/v) PEGDA solutions with relative ratios of pegylated nanotubes to PEGDA of 0, 0.06, 0.1, 0.2, 0.45, and 0.9% (w/w). Irgacure 2959 photoinitiator was dissolved in a 70 : 30 ethanol–water mixture, whereas KPS was dissolved in water. Both initiators were mixed in a 1 : 1 ratio. The mixture was added to the previously prepared precursor solution (SWNT–PEGMA with PEGDA) at a 0.5% (w/w) concentration related to the PEGDA weight. Finally, photocrosslinking was carried out with a 365-nm UV light (Fisher Scientific, Madrid, Spain) at an intensity of 4 mW/cm^2 for 5 min (see Schemes 1 and 2).

Hydrogel characterization

Swelling properties

Following the photopolymerization process described previously, hydrogels 20 mm in diameter and 3 mm in thickness were obtained in polytetrafluoroethylene molds ($n = 6$) for the determination of their swelling properties. For this study, some of the concentrations listed previously were used. As previously established by the Flory–Rehner theory, the wet and dry weights of the samples in a solvent (water) and a nonsolvent (hexane) were obtained, and the swelling properties, such as the volumetric swelling ratio, mass swelling, and equilibrium water content, were determined with the following equations:[42–45]

$$Q = (1 - \phi)\frac{\upsilon_r}{\upsilon_s} \quad (1)$$

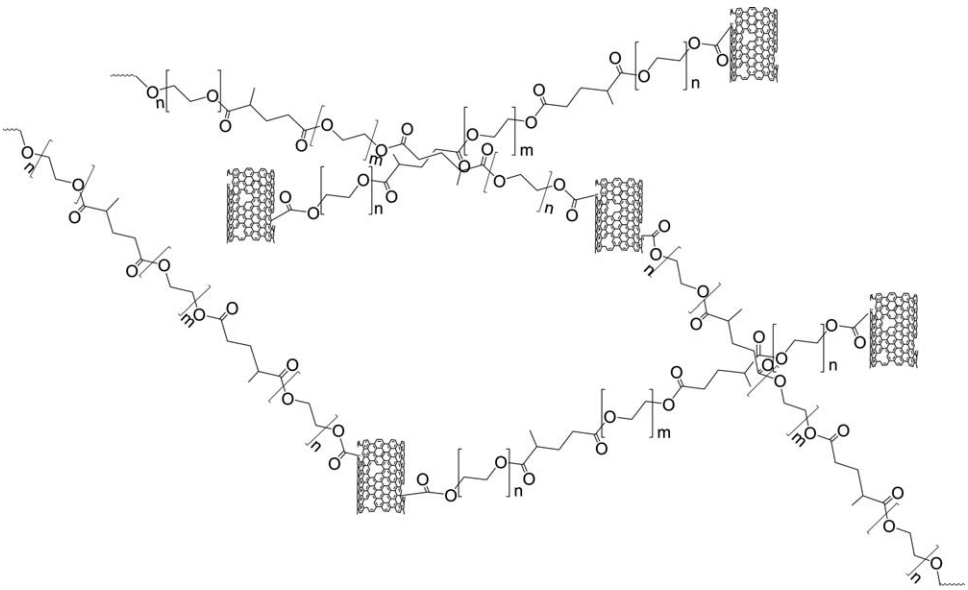

Scheme 2 Scheme of the hybrid SWNT–PEG hydrogel structure.

where Q is the volumetric swelling ratio, ϕ is the solid fraction, and υ_r and υ_s are the volumetric fractions of the polymer in the hydrogel before and after swelling, respectively. These variables can be expressed as follows:

$$\phi = \frac{W_{a,d}}{W_{a,r}}, \quad \upsilon_r = \frac{W_{a,d} - W_{n,d}}{W_{a,r} - W_{n,r}}, \quad \upsilon_s = \frac{W_{a,d} - W_{n,d}}{W_{a,s} - W_{n,s}} \tag{2}$$

where $W_{a,r}$ and $W_{n,r}$ are the weights of the crosslinked hydrogel before swelling in air and hexane (nonsolvent), respectively; $W_{a,s}$ and $W_{n,s}$ correspond to the weights of the crosslinked hydrogel in air and hexane, respectively, after swelling for 24 h; and $W_{a,d}$ and $W_{n,d}$ correspond to the weights of the crosslinked hydrogel in air and hexane, respectively, after swelling for 24 h and then vacuum drying to constant weights. Finally, the equations for the mass swelling (S) and equilibrium water content (EWC) are as follows:

$$S = \frac{W_{a,s} - W_{a,d}}{W_{a,d}} \tag{3}$$

$$\text{EWC} = \frac{W_{a,s} - W_{a,d}}{W_{a,s}} \times 100 \tag{4}$$

Viscoelastic properties

For the measurement of the viscoelastic properties, oscillatory shear rheology was used. Samples 20 mm in diameter and 1 mm in thickness were prepared. Rheological experiments were carried out with parallel-plate geometry (200-mm diameter steel with a gap of 1 mm) of a Thermo Haake Rheostress RS6000 rheometer (Thermo Scientific, Karlsruhe, Germany). Stress amplitude sweeps were performed at a constant frequency of 0.1 Hz to fix the amplitude for each sample and to ensure that subsequent data was collected in the linear viscoelastic regime. All of the measurements were made in constant deformation control mode over a frequency range from 0.01 to 20 Hz. All of the measurements were carried out at room temperature.

Lixiviates characterization

Raman spectroscopy was used to qualitatively analyze the possible desorption of noncovalently attached nanotubes. SWNT–PEG hydrogels (20 × 3 mm) were maintained for 12 days in water under agitation. The solution was then filtered through a GTTP membrane with a 0.2 μm pore size, and the surface of the membrane was analyzed by Raman spectroscopy.

Cytotoxicity assay

The cytotoxicity test of the hydrogels was carried out after a lixiviation process with double-distilled H_2O for 12 days. Cell viability was measured *in vitro* by the culturing of the material with corneal keratocytes and the measurement of the metabolic activity of the cells by a water-soluble tetrazolium salt cell proliferation reagent assay (WST-1 assay, Roche Molecular Biochemicals, Barcelona, Spain). First, keratocytes were isolated from rabbit corneas by a modified sequential collagenase digestion according to an established procedure.[46] Primary cells, pooled from the second and third digestions, were subcultured in a humidified atmosphere of 5% CO_2 at 37°C at a

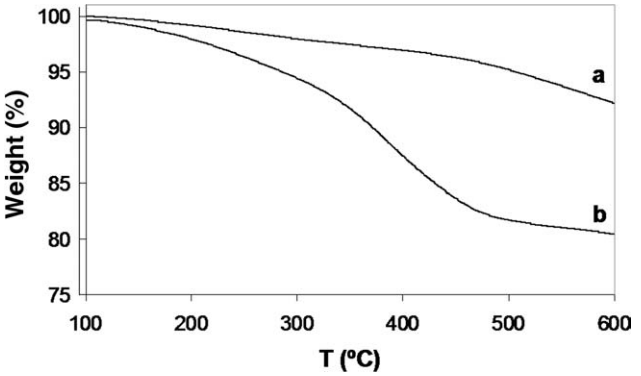

Figure 1 Thermogram curves of the (a) pristine SWNTs and (b) SWNT–PEGMA derivative (T = temperature).

density of 5000 cells/cm^2 in Dulbecco's modified Eagle's medium (DMEM/F12, Invitrogen, Barcelona, Spain) containing 1% antibiotic–antimycotic solution (Invitrogen) and 1% platelet-poor horse serum (Sigma) for 2 days. The serum was then substituted by 10% fetal bovine serum (Sigma), and the culture medium was changed every 2–3 days. When the cells reached approximately 80% confluence, they were trypsinized with trypsin/ethylene diamine tetraacetic acid (Invitrogen) digestion and subcultured with standard methods. After that, the material samples (10 $\times$ 1 mm^2) were placed in culture plates with 3 $\times$ 10^3 keratocytes/sample and the culture medium. After 24 h of culturing, the number of metabolically active cells on the material was quantified by the WST-1 assay according to the manufacturer's protocol. The results were compared with a control sample of PEG hydrogel without SWNT–PEGMA.

RESULTS AND DISCUSSION

CNT functionalization

The well-known acid oxidation treatment of CNTs was performed on the SWNTs to obtain the carboxylated derivative. The extent of the PEGMA esterification in SWNT–PEGMA was further studied by thermogravimetric analysis of the degassed product. Thermogravimetric analysis was useful not only to confirm the SWNT functionalization with PEGMA but also to quantify the extent of it by comparison with the loss of weight of pristine SWNT. Figure 1 shows the loss of weight of pristine SWNTs compared to that of the SWNT–PEGMA intermediate product, which displayed a progressive degradation with a maximum slope at 400°C characteristic of PEGMA. A weight loss of 14% was calculated for the sample at 500°C with the relative degradation of the pristine SWNTs (5%) at such temperature taken into account.

We used X-ray photoelectron spectroscopy to estimate an atomic oxygen percentage of 9 and 26%, on the oxidized SWNT and SWNT–PEGMA samples, respectively. These results confirmed the oxygen enrichment given by the presence of the PEG chain on the SWNT–PEGMA product. Moreover, SEM images provided evidence of SWNTs with a polymer wrapping up to 70 nm. The diameters of the samples corresponding to carboxylated SWNTs were measured by AFM, and we estimated an average value of 10 nm. According to these measurements, covalently attached PEGMA generated a wrapping of 60 nm around the SWNTs (see Fig. 2). These results confirmed the preceding thermogravimetric calculations and strongly suggested the grafting of PEGMA onto the SWNT–CO_2H.

Raman spectroscopy is a valuable characterization method of CNTs because it provides information

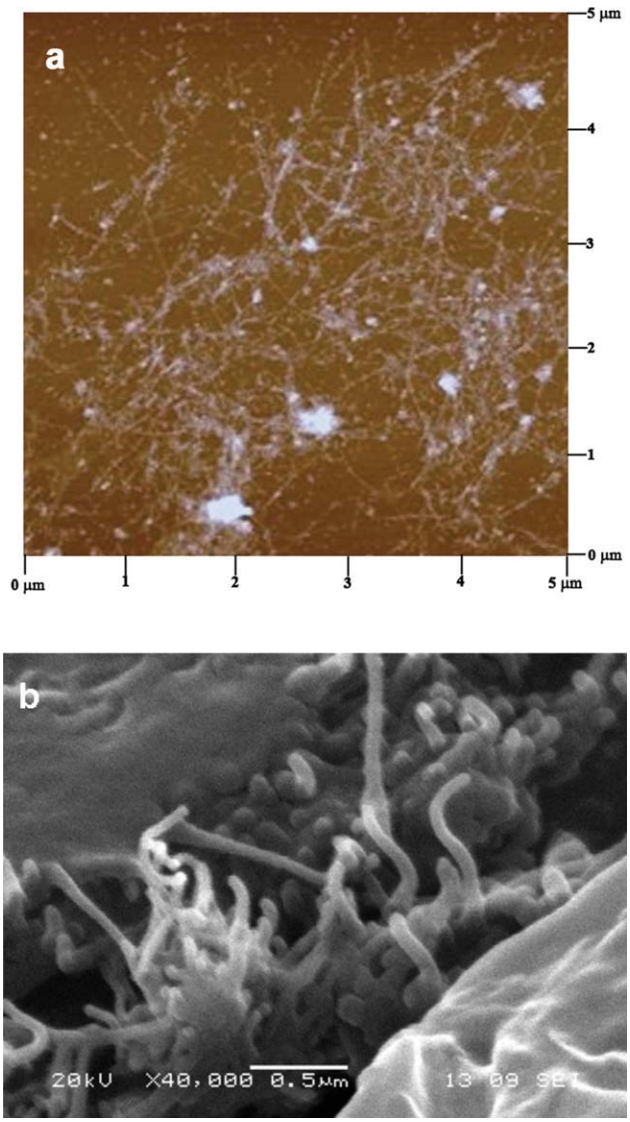

Figure 2 Morphological characterization of (a) SWNT–CO_2H by AFM and (b) SWNT–PEGMA by SEM (magnification = 40,000×). [Color figure can be viewed in the online issue, which is available at wileyonlinelibrary.com.]

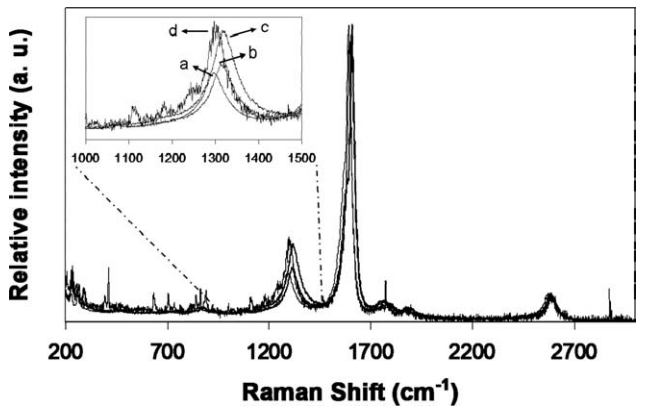

Figure 3 Raman spectra of the (a) pristine SWNTs, (b) nitric acid oxidized SWNTs, (c) sulfuric acid oxidized SWNTs, and (d) SWNT–PEG hydrogels. All spectra were normalized with the G-band intensity.

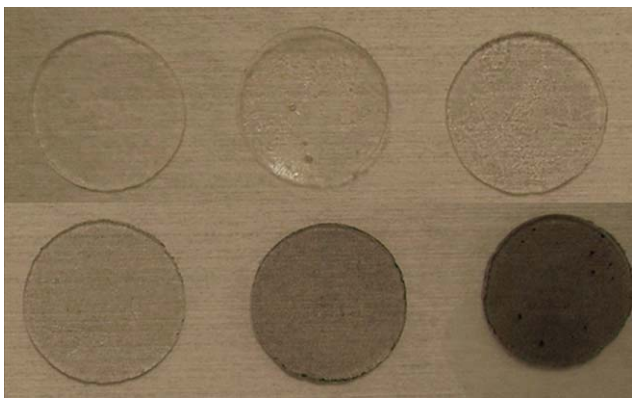

Figure 4 Appearance of hybrid SWNT–PEG hydrogels with SWNT concentrations of 0, 0.06, 0.1, 0.2, 0.45, and 0.9% (w/w). The concentrations increase from left to right and from top to bottom. [Color figure can be viewed in the online issue, which is available at wileyonlinelibrary.com.]

about their structure and properties. It shows how changes in the D band can be used for material characterization to probe and monitor structural modifications of the nanotubes sidewalls, which come from the increment on the carbon sp^3 because of the attachment of different chemical species.[47] Figure 3 shows the Raman spectra of the synthesized derivatives in comparison with the Raman spectrum of pristine SWNTs.

In all cases, three important characteristic features of SWNTs were observed: the tangential G band (at 1595 cm^{-1}), which was derived from the in-plane Raman active mode in graphite; the disorder-induced D band (at 1290 cm^{-1}), and the radial breathing mode peaks at low Raman shifts. The D/G ratio in the pristine SWNTs was 15%. However, in oxidized SWNTs, the D/G intensity relation increased up to 18% in the first nitric acid treatment and to 26% with an additional sulfuric acid oxidation treatment. As expected, the D-band intensity was lower in the pristine SWNTs compared to the oxidized ones and, therefore, the carboxylated SWNTs. The functionalization increased the sp^3 hybridization in the SWNT lattice and, consequently, the disorder-induced D-band intensity. Furthermore, the D/G intensity relation on the SWNT–PEG hydrogel had almost the same value as that of the carboxylated SWNTs and corresponded to 28%. This means that the hydrogel was grown from the carboxyl terminal groups, and no further reactions on the SWNT sidewalls took place.

Hydrogel synthesis and characterization

The scheme of preparation of the hybrid SWNT–PEG hydrogel has been shown in Scheme 2. A dual-initiation system was used to synthesize the hydrogels. It combined a photoinitiator for the UV-exposed areas and a thermal initiator for the underexposed or dark areas, due to the presence of the

TABLE I
Swelling Properties of the Hybrid SWNT–PEG Hydrogels

	Samples with 20% (w/w) PEG			
	20_0	20_0.2	20_0.45	20_0.9
Volumetric swelling	0.72 ± 0.1	0.75 ± 0.1	0.88 ± 0.17	0.92 ± 0.11
Mass swelling	4.70 ± 0.11	4.75 ± 0.09	4.96 ± 0.12	4.75 ± 0.09
Equilibrium water content (%)	82.4 ± 0.3	82.6 ± 0.2	83.2 ± 0.3	82.6 ± 0.3
	Samples with 30% (w/w) PEG			
	30_0	30_0.2	30_0.45	30_0.9
Volumetric swelling	0.78 ± 0.15	0.87 ± 0.25	0.86 ± 0.1	1.01 ± 0.19
Mass swelling	3.74 ± 0.07	3.82 ± 0.02	3.67 ± 0.09	3.66 ± 0.05
Equilibrium water content (%)	78.9 ± 0.3	79.3 ± 0.1	78.6 ± 0.4	78.5 ± 0.2

In the sample nomenclature, the first number is the percentage (w/w) of PEGDA, and the second number is the percentage (w/w) of CNTs.

pegylated nanotubes, which gave opacity to the initial mixture. The appearance of the obtained hydrogels is shown in Figure 4.

Swelling properties

The swelling properties of the synthesized hydrogels are shown in Table I. Each value was the average of six experiments.

The volumetric swelling, mass swelling, and equilibrium water content remained nearly constant in all of the samples for the same PEG content.

Usually, swelling parameters (volumetric swelling, mass swelling, and equilibrium water content) are mainly dependent on the PEG concentration for a constant molecular weight,[48] and as we observed, the hydrogels of 20% PEGDA showed higher values than those of 30% PEGDA. This was due to the fact that the amount of polymer chains in the network increased with the concentration of PEG; this decreased the free volume available inside the polymer network and the amount of water the hydrogel could take up when hydrated. The swelling properties of the hydrogel were not strongly affected by the presence of the pegylated nanotubes.

After this analysis, the 30% PEG composition was chosen to study the influence of the percentage of nanotubes in the hydrogel behavior because no strong differences in the hydrogel characteristics were observed when the PEG content was changed, apart from those predicted by the Flory–Rehner theory.

Viscoelastic properties

The viscoelastic properties of the hydrogel were obtained by a rheological study. Small-deformation oscillatory measurements were used to evaluate the viscoelastic behavior of the hydrogels and to study the effects of SWNTs on the hydrogel strength. The amplitude or strain selected for each sample was 0.075 for gels with 0%, 0.09 for those with 0.06%, 0.6 for those with 0.1%, and 0.12 for those with 0.2% SWNTs. After this, frequency scanning at a constant amplitude was done for each sample.

Figure 5 displays the viscoelastic properties of gels with pegylated SWNTs that ranged from 0 to 0.2% (w/w), but the experiment was also done for higher amounts (0.45 and 0.9% w/w, for which the data are not shown).

As shown in Figure 5, the native PEG hydrogels without SWNTs showed higher storage modulus (G') values than loss modulus (G'') values over the entire range of frequencies; this indicated a predominance of the elastic behavior over the viscous behavior; this is an intrinsic characteristic of hydrogels. In the case of hydrogels with nanotubes, we observed

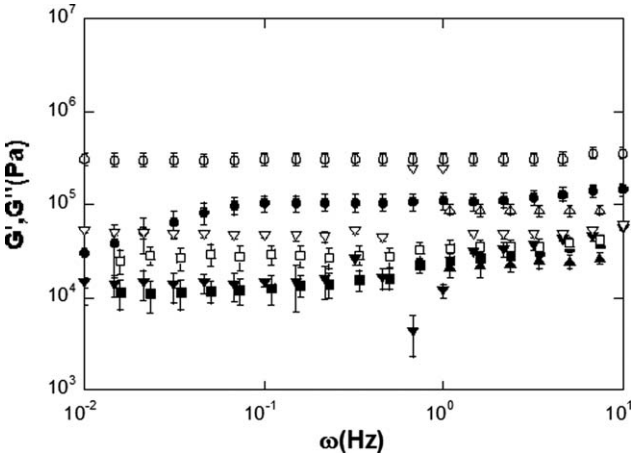

Figure 5 Dynamic rheological behavior of the native and hybrid hydrogels with 0% (w/w) SWNTs [(●) G'' and (○) G'], 0.06% (w/w) SWNTs [(■) G'' and (□) G'], 0.1% (w/w) SWNTs [(▲) G'' and (△) G'], and 0.2% (w/w) SWNTs [(▼) G'' and (▽) G']. ω = frequency.

that the viscoelastic properties decreased when they were compared with the hydrogel without nanotubes. The samples showed $G' > G''$; this is characteristic of elastic materials such as hydrogels, but the moduli were smaller than those of native PEG and showed the influence of the nanotube presence on the material elasticity. When we compared the hybrid systems to each other, we concluded that their behaviors were very similar. No better results could be obtained at higher amounts of SWNTs (data not shown); the bad results for the higher SWNT percentages (0.45 and 0.9% w/w) could have been due to the loss of gel nature, where the nanotubes made it behave as a more brittle material, which was impossible to measure correctly.

All these results indicate that the mechanical properties were not improved by the SWNTs. The same result was reported previously by other researches.[28] This behavior could have been due to the fact that the nanotubes might have affected the crosslinking process of the polymer chains and led to some inhomogeneities and defects in the network on the nanometric scale, with somewhat lower crosslinking density. When the nanotubes were added, the crosslinking density decreased, and such a decrease was manifested by a slight increase in the swelling and a drop in the G' values.

Somehow, the nanotubes could have influenced the elastic nature of the original hydrogel and changed its viscoelastic behavior under stress, as shown before by an increase in the breakability of the material.

Lixiviates characterization

With the aim to explore the presence of nonbounded SWNTs in lixiviates after several days of incubation,

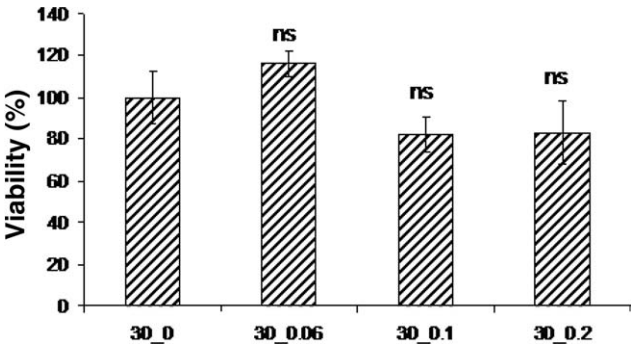

Figure 6 Cell viability (%) after cell culturing with the native and hybrid hydrogels with 0.06, 0.1, and 0.2% (w/w) SWNTs. ns indicates data that are not significant with respect to the control (30_0).

the solutions were passed through a polycarbonate membrane. After each washing, some isolated black spots were observed on the membrane, which decreased as the time of washing increased. We used Raman spectroscopy to provide structural characterization of those black spots, focusing the laser beam by coupled optical microscopy. The obtained SWNT characteristic Raman spectra, similar to those shown in Figure 3(d), demonstrated the release of the nanomaterial.

These results indicate that it was probable that the reaction of covalent attachment between the PEGMA of the nanotubes and the PEGDA during the formation of the hydrogel network did not reach yields of 100%, probably because of the fact that even with the dual initiation, there were some blind points where the reaction did not take place properly. Most of these small amounts of nonreacted SWNTs were released during a period of 12 days of washing.

Cytotoxicity evaluation

Cytotoxicity tests represent the initial step in testing the biocompatibility of potential biomaterials. After the samples were washed for 12 days and after they were cultured for a 24 h, quantitative WST-1 analysis was used to determine the viable number of cells after the contact. The cytotoxicity ratios of the tested materials were calculated from the average optical density values measured at the standardized wavelength established in the WST-1 assay. The results shown in Figure 6 are reported as the average plus or minus the standard deviation and with statistical analysis with the Student t test ($p > 0.05$, $p \geq 0.01$, and $p \geq 0.001$) and refer to the control of the PEG hydrogel without nanotubes.

The results show a slight increase in the number of viable cells when keratocytes were cultured on the hydrogels with a lower amount of SWNT (0.06%) and a slight decline with higher concentrations of SWNTs (0.1 and 0.2%) with respect to the hydrogel control without SWNTs. These small differences were not statistically significant with respect to the control, with all of them close to 100% viability, so the composite hydrogels were considered noncytotoxic; this demonstrated that they had good cell biocompatibility.

For future applications, it would be desirable to avoid any kind of cytotoxic effect. Therefore, more studies will be needed to adjust the limit of SWNT concentration and to improve the prewash treatment to purify the material from the nonreacted subproducts.

CONCLUSIONS

This article demonstrates a new and simple method to hybridize SWNTs into a hydrogel by a previous functionalization of SWNTs with PEGMA. The pegylated nanotubes were covalently bound through their PEG moieties to a PEG hydrogel network, which came from the crosslinking reaction of the PEGDA prepolymer. The hybrid hydrogels were then synthesized by dual photo-UV and thermal initiations. Their swelling properties were maintained when they were compared with the native PEG hydrogel. However, the network properties changed because of the presence of the pegylated nanotubes. Their mechanical properties also declined slightly. In addition, the material and lixiviates were analyzed, and their cytotoxicity was studied; we concluded that in the assayed concentrations, these hybrid materials were nontoxic.

The authors thank El Centro de Investigación Biomédica en Red en Bioingeniería, Biomateriales y Nanomedicina (San Sebastián, Spain) and Jesus Merayo and coworkers at the Institute of Applied Ophthalmobiology (Valladolid, Spain).

References

1. Prato, M.; Kostarelos, K.; Bianco, A. Acc Chem Res 2008, 41, 60; (b) Foldvari, M.; Bagonluri, M. Nanomedicine 2008, 4, 183.
2. Moniruzzaman, M.; Sahin, A.; Winey, K. I. Carbon 2009, 47, 645.
3. Ajayan, P. M.; Tour, J. M. Nature 2007, 447, 1066.
4. Ruoff, R. S.; Qian, D.; Liu, W. K. C. R. Phys 2003, 4, 993.
5. Pascual, B.; Castellano, I.; Vázquez, B.; Gurruchaga, M.; Goñi, I. Polymer 1996, 37, 1005.
6. Karadag, E.; Saraydin, D.; Cetinkaya, S.; Guven, O. Biomaterials 1996, 17, 67.
7. Drury, J. L.; Mooney, D. J. Biomaterials 2003, 24, 4337.
8. Park, H.; Temenoff, J. S.; Holland, T.; Tabata, Y.; Mikos, A. G. Biomaterials 2005, 26, 7096.
9. Rafat, M.; Li, F.; Fagerholm, P.; Lagali, N. S.; Watsky, M. A.; Munger, R.; Matsuura, T.; Griffith, M. Biomaterials 2008, 29, 3960.
10. Xingiao, J.; Kiik, K. L. Macromol Biosci 2009, 9, 140.
11. Han, J.; Wang, K.; Yang, D.; Nie, J. Int J Biol Macromol 2009, 44, 229.
12. Katime, I.; Sáez, V.; Hernáez, E. Polym Bull 2005, 55, 403.

13. Namba, R. M.; Cole, A. A.; Bjugstad, K. B.; Mahoney, M. J. Acta Biomater 2009, 5, 1884.
14. Wnek, G. E.; Bowlin, G. L. In Encyclopedia of Biomaterials and Biomedical Engineering, 2nd ed.; Wnek, G. E.; Bowlin, G. L., Eds.; Informa Health Care: New York, 2008.
15. Lee, K. Y.; Mooney, D. J. Chem Rev 2001, 101, 1869.
16. Peppas, N. A.; Keys, K. B.; Torres-Lugo, M.; Locuman, A. M. J Controlled Release 1999, 62, 81.
17. Harris, J. M. Chemistry Biotechnical and Biomedical Applications; Plenum Press: New York, 1992; p 1.
18. Cruise, G. M.; Scharp, D. S.; Hubell, S. A. Biomaterials 1998, 19, 1987.
19. West, J. L.; Hubbell, S. A. Macromolecules 1999, 32, 241.
20. Bryant, S. J.; Anseth, K. S. Biomaterials 2001, 22, 619.
21. Jung, D.; Ko, Y.; Jung, H. Mater Sci Eng C 2004, 24, 117.
22. Zhou, B.; Lin, Y.; Li, H.; Huang, W.; Connell, J. W.; Allard, L. F.; Sun, Y. J Phys Chem B 2003, 107, 13588.
23. Kitaygorodskiy, A.; Wang, W.; Xie, S.; Lin, Y.; Fernando, S.; Wang, X.; Qu, L.; Chen, B.; Sun, Y. J Am Chem Soc 2005, 127, 7517.
24. Olalde, B.; Aizpurua, J. M.; Garcia, A.; Bustero, I.; Obieta, I.; Jurado, M. J. J Phys Chem C 2008, 112, 10663.
25. Sabba, Y.; Thomas, E. L. Macromolecules 2004, 37, 4815.
26. Li, H.; Wang, D. Q.; Chen, H. L.; Liu, B. L.; Gao, L. Z. Macromol Biosci 2003, 3, 720.
27. Asai, M.; Sugiyasu, K.; Fujita, N.; Shinkai, S. Chem Lett 2004, 33, 120.
28. Wang, Z.; Chen, Y. Macromolecules 2007, 40, 3402.
29. Tong, X.; Zheng, J.; Lu, Y.; Zhang, Z.; Cheng, H. Mater Lett 2007, 61, 1704.
30. Qian, D.; Dickey, E. C.; Andrews, R.; Rantell, T. Appl Phys Lett 2000, 76, 2868.
31. Bower, C.; Rosen, R.; Jin, L.; Han, J.; Zhou, O. Appl Phys Lett 1999, 71, 3317.
32. Ajayan, P. M.; Schadler, L. S.; Giannaris, C.; Rubio, A. Adv Mater 2000, 12, 750.
33. Kong, H.; Gao, C.; Yan, D. J Mater Chem 2004, 14, 1401.
34. Chattopadhyay, J.; Cortez, F.; Chakraborty, S.; Slater, N. K. H.; Billups, W. E. Chem Mater 2006, 18, 5864.
35. Chen, J.; Xue, C.; Ramasubramaniam, R.; Liu, H. Carbon 2006, 44, 2142.
36. Burdick, J. A.; Peterson, A. J.; Anseth, K. S. Biomaterials 2001, 22, 1779.
37. Studer, K.; Decker, C.; Beck, E.; Schwalm, R. Eur Polym J 2005, 41, 157.
38. (a) Rinzler, A. G.; Liu, J.; Dai, H.; Nikolaev, P.; Huffman, C. B.; Rodríguez Macías, F. J.; Boul, P. J.; Lu, A. H.; Heymann, D.; Colbert, D. T.; Lee, R. S.; Fischer, J. E.; Rao, A. M.; Eklund, P. C.; Smalley, R. E. Appl Phys A 1998, 67, 29; (b) Liu, J.; Rinzler, A. G.; Dai, H. J.; Hafner, J. H.; Bradley, R. K.; Boul, P. J.; Lu, A.; Iverson, T.; Shelimov, K.; Huffman, C. B.; Rodriguez--Macias, F.; Shon, Y. S.; Lee, T. R.; Colbert, D. T.; Smalley, R. E. Science 1998, 280, 1253.
39. Chen, J.; Hamon, M. A.; Hu, H.; Chen, Y. S.; Rao, A. M.; Eklund, P. C.; Haddon, R. C. Science 1998, 282, 95.
40. Bryant, S. J.; Anseth, K. S. J Biomed Mater Res 2002, 59, 63.
41. Bryant, S. J.; Anseth, K. S.; Lee, D. A.; Bander, D. L. J Orthop Res 2004, 22, 1143.
42. Flory, P. J.; Rehner, J. J Chem Phys 1943, 11, 521.
43. Flory, P. J. In Principles of Polymer Chemistry; Cornell University Press: Ithaca, NY, 1953
44. Temenoff, J. S.; Athanasiou, K. A.; LeBaron, R. G.; Mikos, A. G. J Biomed Mater Res 2002, 59, 429.
45. Peppas, N. A.; Barr-Howell, B. D. In Hydrogels in Medicine and Pharmacy; CRC: Boca Raton, FL, 1986; p 27.
46. Beales, M. P.; Funderburgh, J. L.; Jester, J. V.; Hassell, J. R. Invest Ophthalmol Vis Sci 1999, 40, 1658.
47. Dresselhaus, M. S.; Dresselhaus, G.; Saito, R.; Jorio, A. Phys Rep Rev Sec Phys Lett 2005, 409, 47.
48. Cruise, G. M.; Scharp, D. S.; Hubbell, J. A. Biomaterials 1998, 19, 1287.